IOPscience iopscience.iop.org

Home Search Collections Journals About Contact us My IOPscience

Amorphous organic devices—degenerate semiconductors

This article has been downloaded from IOPscience. Please scroll down to see the full text article.

2002 J. Phys.: Condens. Matter 14 9913

(http://iopscience.iop.org/0953-8984/14/42/306)

View the table of contents for this issue, or go to the journal homepage for more

Download details:
IP Address: 171.66.16.96
The article was downloaded on 18/05/2010 at 14:56

Please note that terms and conditions apply.

INSTITUTE OF PHYSICS PUBLISHING JOURNAL OF PHYSICS: CONDENSED MATTER

J. Phys.: Condens. Matter **14** (2002) 9913–9924 PII: S0953-8984(02)37130-3

Amorphous organic devices—degenerate semiconductors

Yevgeni Preezant, Yohai Roichman and Nir Tessler

Electrical Engineering Department, Technion Israel Institute of Technology, Haifa 32000, Israel

Received 17 May 2002
Published 11 October 2002
Online at stacks.iop.org/JPhysCM/14/9913

Abstract
The device-physics features of organic materials are presented from an engineering point of view. By treating the organic material and the device in a self-consistent manner the unique features of organic devices are revealed. We discuss charge injection and transport relevant to (polymer/small molecule) light-emitting diodes and field-effect transistors.

(Some figures in this article are in colour only in the electronic version)

1. Introduction

Charge injection and transport phenomena have been studied for many years and in many material systems [1, 2] including that of organic semiconductors [3–6]. Many of these studies are now being revisited [5, 7–12], as high-quality devices seem to emerge through the use of new and better material [13]. Moreover, lately these materials have become commercially available, thus opening the field to many research groups. Nevertheless, the field of organic devices is still largely driven by the evolution and invention [14] of new materials and materials composites [15, 16]. From the device-physics point of view this implies that one should constantly consider a range of mechanisms in order to decide which (set) is most suitable ('intrinsic') to describe the material under study. This above point is not only due to the conjugated organic materials being 'on the move' but also due to them not being strictly categorized, as the inorganic ones often are. Having the above in mind the purpose of this paper is to consider mechanisms or phenomena that are more likely to occur in devices based on materials available today. We limit ourselves to devices which are either light-emitting diodes (LEDs) or field-effect transistors (FETs). In order to appeal to a wider audience we also attempt to provide some background before presenting a few results. One of the main messages arising from our study is that the mechanisms underlining the organic-material-based device operation or the equations describing them are complex and non-linear.

The materials in question are known either as conjugated molecules (polymers) or as organic semiconductors. The second term is more widely appealing; however, it sometimes leads to confusion as one would be tempted to apply the very well established knowledge and know-how of semiconductors (inorganic) and not consider the molecular nature of these

 © 2002 IOP Publishing Ltd Printed in the UK

materials. Just as one should apply special treatment or even terminology to quantum dots [17] with respect to bulk crystalline materials, one should do the same with respect to molecular materials (semiconductors). Namely, before applying a model/expression to describe the performance of an organic device one should not only verify that the model is well established but also that the details of the physical picture that underlie it can be fitted to organic materials (as are known today).

To understand (reveal) the basic unique features of amorphous organic semiconductors one often looks at the system dynamics through either Monte Carlo or statistical methods [6, 18]. In contrast to these, our goal here is to examine device-oriented phenomena and we assume, *a priori*, that quasi-equilibrium is established faster then the timescale of interest. Before doing so and as a matter of introduction we mention one of the features that has been established via the use of dynamic methods—the dispersive transport. The term dispersive (non-equilibrium) transport is often used in cases where the motion of the charges cannot be defined using only two moments (D and μ) or, in other words, in cases where the mobility (μ) is an ill defined concept [6, 19]. Such situations usually occur when the excitations continue to relax towards a quasi-equilibrium state during the entire observation time [5, 6, 19, 20]. In the case of charge excitation the observation time is usually the time taken to transport across the device under test. Namely, the shorter the device (or the timescale) the more likely it is to encounter the dispersive transport phenomena, and by varying the device length (timescale) one may also find a transition from dispersive (relaxation or non-equilibrium) transport to non-dispersive transport [5, 21]. Extensive discussion of dispersive versus non-dispersive transport [5, 19, 20, 22–26] is beyond the scope of this paper and we only wish to emphasize that the experimental observation of one or the other is not only material dependent but also experimental-detail dependent (mainly temperature-dependent timescales and/or spatial dimensions).

The sophisticated methods mentioned above are often applied within the low-density limit [6, 18] so that the following hold.

(1) Boltzmann statistics can be used instead of Fermi–Dirac (FD).
(2) No blocking effects associated with state filling are present.
(3) Space charge effects are negligible.

Such low density may be found at the front tail of a charge distribution in a transient time-of-flight measurement [27] or in transient light emission in LEDs. Beyond this transient edge it is most likely that the low-density limit does not hold. Indeed, different conclusions have been drawn when a mobility value was extracted from the charge-distribution front end (light turn-on) [24] or when the body of the charge distribution (high-density part) was used [11]. The first method showed that the low-density charge-carrier front was subject to relaxation effects (dispersive effects) and hence a true mobility could not be derived. When the body of the charge distribution (high-density part) was used, a meaningful mobility value could be extracted in either the time [11] or frequency [28, 29] domains. Namely, there is a real motivation to look into density-related effects [30] in organic materials.

2. The physical picture

From the above introduction it is clear that one should attempt to use semiconductor device models. However, it is well established that charge transport in disordered semiconductors is not fully characterized by the conventional current continuity equations [5, 6, 22]. In the context of organic semiconductors, it is accepted that the mobility is exponential in the square root of the electric field [31]; however, this modification is also often found to be insufficient. The deviation of the experimental results from the conventional current continuity equation

description is typically explained either in the context of transport under non-equilibrium conditions [19, 21] or with the aid of detailed Monte Carlo simulations [32] of hopping transport. As already stated, a common feature of these detailed studies in that they do not consider (or even preclude) effects associated with the charge density.

To introduce density-dependent effect we perform quasi-steady-state (or quasi-equilibrium) analysis based on the shape of the density of states (DOS) being Gaussian, as described in numerous papers by Bassler and co-workers [5, 18, 33, 34]. To this we add two assumptions:

(1) the transport can be described using two moments only (mobility and diffusion coefficients) and
(2) the charges are at quasi-equilibrium (no energy/momentum equation needed).

We start by examining whether such a semiconductor is non-degenerate or degenerate [30]. Namely, we examine whether one must use the full FD statistics

$$\mathrm{FD} = \frac{1}{1 + \exp\left(\frac{E-E_\mu}{kT}\right)},$$

or whether it is sufficient to use the simpler form of the Boltzmann (Bz) statistics,

$$\mathrm{Bz} = \exp\left(-\frac{E - E_\mu}{kT}\right).$$

To do so we plot in figure 1 the charge density (solid curve) as a function of the position of the chemical potential or quasi-Fermi level (E_μ) relative to the centre of the Gaussian DOS ($\sigma = 7kT$) as calculated using the FD expression. For reference, the exponential decay (as in Boltzmann statistics) is shown as a dashed line. The shape of the DOS is also shown (dotted curve, right axis). We note that only when the excitation density is as low as 10^{-10} of the effective DOS does the slope approach that expected from a Boltzmann factor.

Another way of looking at degeneracy or non-degeneracy is to plot the excitation (charge) energy distribution as a function of the energy position of the chemical potential. In the non-degenerate case the excitation energy distribution should be well separated from the chemical potential. Figure 2 presents the energy distribution of charge carriers residing in a material having a Gaussian DOS with a width $\sigma/kT = 3$. Again, the calculation is performed as a function of the position of the quasi-Fermi level (chemical potential) relative to the centre of the DOS. We note that as the quasi-Fermi level is lowered (charge density becomes lower), the energy of the centre of the charge distribution goes down and saturates at a value of $\langle E_{N\to 0}\rangle/kT = (\sigma/kT)^2 = 9$. Only when the quasi-Fermi level is well below this saturation energy can one treat the material as non-degenerate and approximate the distribution using Boltzmann statistics. It is interesting to note that figure 2 of this paper agrees well with figure 2 in [18], where the time evolution of the charge energy distribution is shown to converge to a value of $\langle \varepsilon_\infty\rangle/kT = (\sigma/kT)^{2}$. This is a first indication that our approach extends the low-density methods to the high-density regime (when strong effects of the electric field can be neglected). Using a calculation as in figure 2, one can deduce the maximum density that is still within the low-density limit (N_{max}). For $\sigma = 3kT N_{max} \approx 5\times 10^{16}$ cm^{-3} and for $\sigma = 7kT N_{max} = 10^7$ cm^{-3}, assuming an effective DOS $N_{eff} = 10^{20}$ cm^{-3}. In other words, high-density effects may occur, in practical devices/materials, at rather low densities, well before space–charge effects come into play. Namely, at all practical densities the amorphous organic semiconductor is degenerate and the use of the Boltzmann factor is not strictly valid. As we show below, this has an impact on charge transport and charge injection in devices.

We start by examining the charge transport and more specifically the phenomena of anomalous spreading. As spreading is generally associated with diffusion we start by

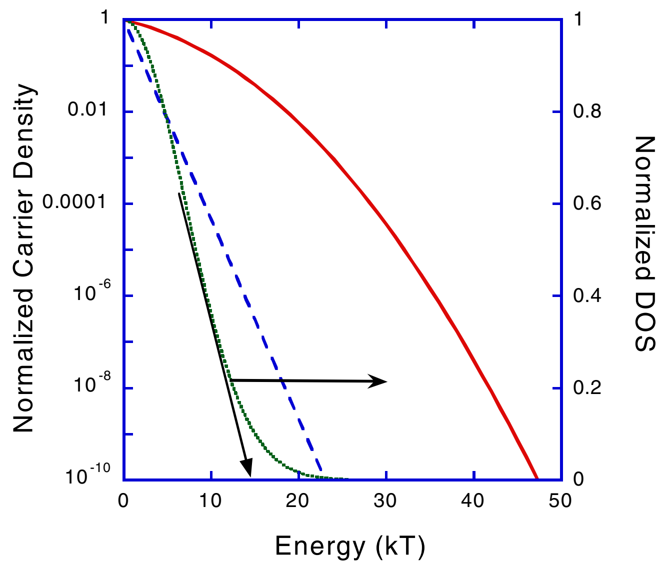

Figure 1. The normalized excitation density (solid curve) as a function of the energetic position of the chemical potential. The dashed curve represents the slope expected from a Boltzmann factor. For orientation, the shape of the DOS is also shown (dotted curve, right axis). The arrow drawn parallel to the DOS shape illustrates the energy at which the DOS becomes more pronounced.

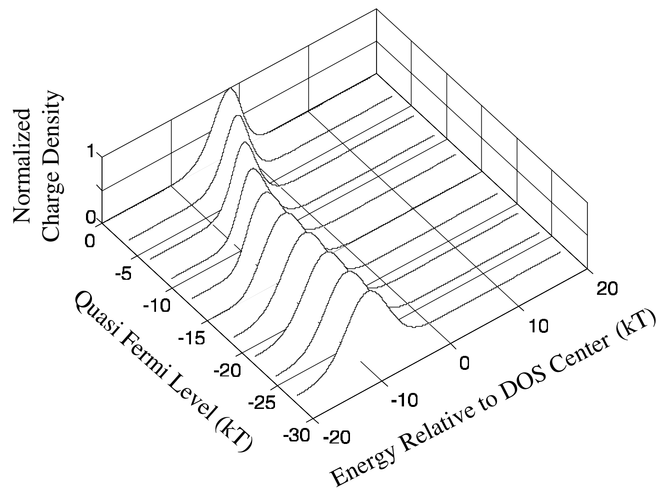

Figure 2. The normalized charge density distribution as a function of energy for different quasi-Fermi levels (chemical potentials). The DOS is Gaussian with $\sigma = 3kT$.

examining the generalized Einstein relation [2] using the appropriate DOS. The derivation starts with the current-transport equation

$$J_h = \mu_h n_h E - D_h \frac{\mathrm{d}}{\mathrm{d}x} n_h. \tag{1}$$

Assuming no external force ($J_h = 0$), one can derive $\mu_h = D_h \frac{1}{n_h} \frac{\mathrm{d}n_h}{E\,\mathrm{d}x} = -D_h \frac{1}{n_h} \frac{\mathrm{d}n_h}{\mathrm{d}V}$. Since we have already required the existence of quasi-equilibrium we can replace the voltage difference

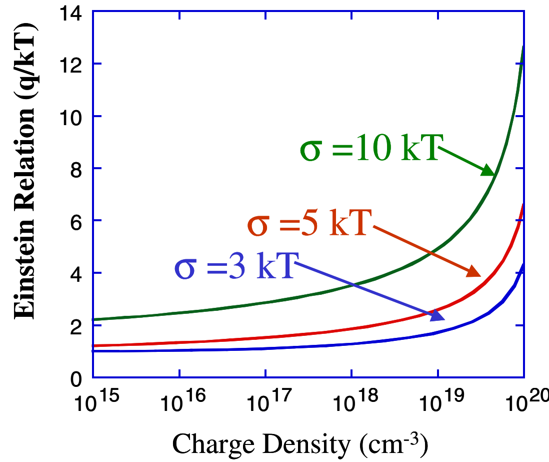

Figure 3. The factor by which the classical Einstein relation is enhanced as a function of charge density assuming three different widths of the Gaussian DOS.

with the difference in the quasi-Fermi-level (chemical potential) position and arrive at the generalized Einstein relation:

$$\mu_h = -D_h \frac{1}{n_h} \frac{\mathrm{d}n_h}{\mathrm{d}E_f}. \tag{2}$$

It can be shown that whenever one can use the Boltzmann statistics to describe the charge energetic distribution (low-density limit or non-degenerate limit), the original Einstein relation $\mu_h = D_h \frac{q}{kT}$ is recovered [2]. When the Boltzmann statistics is not a good enough approximation and one must use the FD statistics (high-density or degenerate limit), then the product $\frac{1}{n_h}\frac{\mathrm{d}n_h}{\mathrm{d}E_f}$ must be re-evaluated [2].

A calculation based on equation (2) is shown in figure 3, where the factor by which the ratio between diffusion and mobility coefficient is larger then kT/q is plotted as a function of the carrier density ($N_{eff} = 10^{20}$ cm^{-3}). The DOS was assumed to be Gaussian and three different Gaussian widths were considered [35], representing three different degrees of disorder [5, 25]. We note that a semiconductor having a Gaussian DOS with a width of 100 meV is considered degenerate at all practical densities (at room temperature). This effect (degeneracy) is most pronounced near interfaces where charges tend to accumulate to high densities. One such interface is the injection contact found in LEDs and another such interface is the gate–insulator boundary found in FET configurations. We note that for such cases the ratio can be up to an order of magnitude higher, thus proportionally enhancing the charge distribution width (channel width in FETs). The more fundamental impact is that the transport equations are highly non-linear (with the charge density), and hence theoretical treatments based on Green-function analysis [36] (impulse response) have to be revisited.

An Einstein relation much higher than one has already been suggested before through Monte Carlo simulations [27, 34] where the statistics of the device/material are built in a dynamic fashion. We believe that under equilibrium conditions our approach extends the statistics of the Monte Carlo simulations from the low-density limit to the high densities used in the devices considered here. Taking into account the results of figure 3, we propose that ‘anomalous’ spreading is largely due to high-density effects and not necessarily due to non-equilibrium effects. To test this hypothesis, we have simulated a time-of-flight measurement where a light pulse is used to create a charge packet close to one contact and its motion through the device is

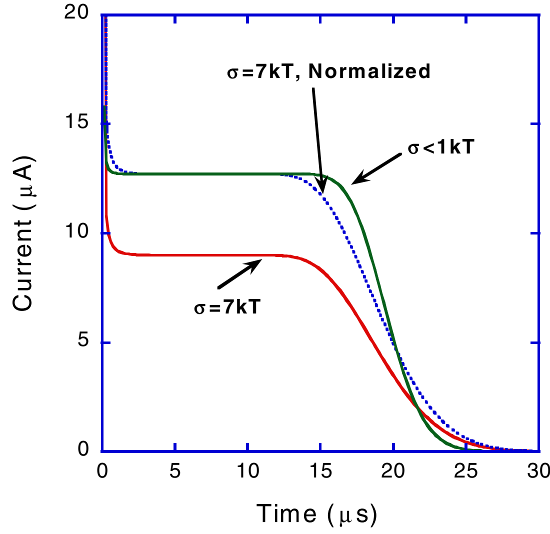

Figure 4. The calculated current response to a light pulse in a time-of-flight experiment. The device length is 1 μm, its cross section is 1 mm^2, the applied reverse bias is 5 V and the mobility $\mu = 10^{-6}$ cm^2 V^{-1} s^{-1}. The top solid curve was calculated for a narrow DOS and the bottom solid curve for a wide DOS ($\sigma = 7kT$ at RT). The dotted curve is the $\sigma = 7kT$ curve normalized to the $\sigma < 1kT$ curve.

monitored via the current. Figure 4 shows such a calculation, where the current response is plotted for two DOS widths. We note that for the wider DOS there is a pronounced decay near $t = 0$ and a broadened decay at the end of the response. These two features, derived under equilibrium conditions, are in good agreement with those reported through Monte Carlo simulations.

3. Implications for device operation

3.1. The space-charge-limited model at the injection interface

To examine the effect on LEDs we first revisit the known model, that is often applied to organic light-emitting devices, of the space-charge-limited (SCL) [9, 10, 37, 38] conduction. The conditions for the SCL model to hold require that the injected charge density near the contact is high enough to screen the applied electric field near the contact. As most (non-contaminated) conjugated materials are intrinsic, or contain a negligible amount of charge density at zero applied voltage, it is very likely that the SCL conditions will hold for reasonably good contact materials. Under these conditions, and assuming that the diffusion currents are negligible, the analytic form of the SCL follows the Mott–Gurney relation [1]:

$$J_{SCL} = \frac{9}{8}\varepsilon\mu\frac{V^2}{d^3}. \tag{3}$$

Here d is the device thickness (distance between contacts), V is the net applied voltage (the applied minus the built in), ε is the permittivity and μ is the mobility. Within this framework the electric field in the device follows [1]

$$E(x) = \sqrt{\frac{2J_{SCL}}{\varepsilon\mu}(x + K)} \tag{4}$$

where x is the distance from the contact and K is given by $K = \frac{J_{SCL}\varepsilon}{2N_0^2e^2\mu}$ with N_0 being the injected charge density at the contact. When N_0 is large enough K tends towards zero and the SCL current–voltage relation holds. When equation (1) is valid the electric field at the other contact reaches a maximum of $E_{max} = 1.5\frac{V}{d}$. In practice equation (1) holds as long as $K \ll d$. If, however, N_0 is low (as in the case of high injection barrier), one may arrive at the other extreme of $K \gg d$, where the electric field becomes constant throughout the device and current–voltage relations become ohmic-like, and the current is then directly proportional to the mobility $J_{ohm} = N_0e\mu\frac{V}{d}$. In the organic device community it is common to name the regime where $K \ll d$ bulk-limited conduction and that where $K \gg d$ injection limited. Using the above relations, developed in [1], one can show that bulk-limited conduction occurs when

$$\frac{J_{SCL}\varepsilon}{2e^2\mu} \ll dN_0^2 \tag{5}$$

or

$$\frac{9V^2\varepsilon^2}{16d^4e^2} \ll N_0^2. \tag{6}$$

From the above we note that the maximum allowed barrier height is bias dependent (V), device dependent (d), temperature dependent (kT) and material dependent. If we use the Boltzmann approximation of

$$N_0 \cong N_{eff}\exp\left(-\frac{\Delta}{kT}\right) \tag{7}$$

and assume $V = 10$ V, $d = 100$ nm, $kT = 0.026$ and $N_{eff} = 10^{21}$ cm^{-3}, we find that for the SCL current–voltage relation to hold $\Delta < 0.43$ eV. For a Gaussian DOS this would correspond to the contact Fermi level being ~0.9 eV ($35kT$) below the centre of the Gaussian (assuming $\sigma = 7kT$ as in figure 1). If one requires to be consistent with the simplified approach that places the limit at about 0.43 eV below a band-edge one may use the asymptotic arrow in figure 1 to define an 'edge' at about 0.4 eV (~2σ) below the Gaussian centre. We do not rigorously justify such an edge position and it is done only for illustration purposes, though it is similar to the method applied to absorption spectrum or STM measurements [39].

An interesting point to make with respect to the SCL treatments is that the result in equation (4) shows that very close to the contact the electric field is negligible and hence the current must be diffusive. Namely, the basic assumption used to derive the SCL relation does not hold near the contact as the diffusion current is the main conduction mechanism at the contact interface (contact is diffusion controlled!?). In large devices ($d \gg 1$ μm) the specifics of the contact may probably be neglected. As most organic LEDs are only 100 nm thick, it is not obvious that one can neglect the contact details. As there exists a wide spread in the energy position of the conduction levels in organic polymers/molecules (see figure 5), the effect of the contact or the energy barrier may become most important. To better understand the applicability of the SCL theory we perform a numerical simulation [11, 40, 41] (minimal assumptions) of a single-carrier charge injection device. The assumed charge density at the contact is $N_0 = 10^{19}$ cm^{-3}, so $K \ll d$.

Figure 6(a) describes charge (hole) density distribution and figure 6(b) describes the internal field and internal potential distribution for an applied voltage of $V_{Appl} - V_{bi} = 1$ V (i.e. $V_{Appl} = 3$–4 V). The solid curves were calculated assuming $D = \frac{kT}{q}\mu$ and the dotted curves were calculated taking into account the effects of the Gaussian DOS ($\sigma = 7kT$) as discussed in the text regarding figure 3. Figure 6(b) clearly shows that equation (2) does not hold in the vicinity of the injection interface. Near the interface, the high charge density (figure 6(a)) causes a negative electric field to be present, which gives rise to a potential barrier

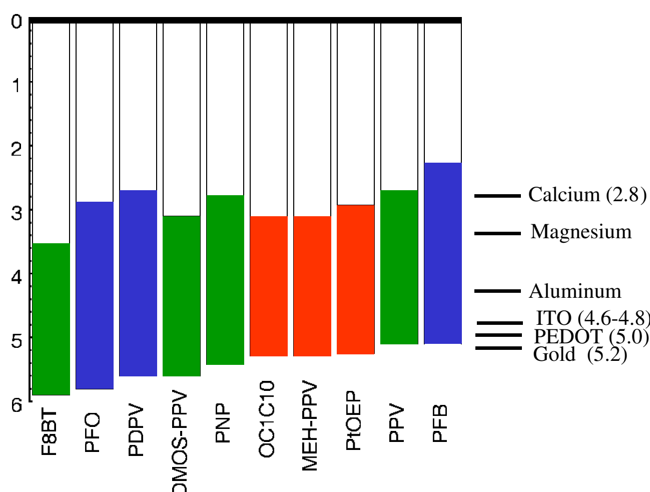

Figure 5. Illustrative description of the estimated position of the HOMO (hole) and LUMO (electron) levels relative to the vacuum level and the corresponding bandgap for a range of polymers. The top of each bar is the LUMO level, the bottom is the HOMO level and its length is the bandgap. For reference the work function of some contact materials is also shown.

that peaks at $x_{max} \sim 10$ nm (15 nm for dotted line) away from the interface. Beyond this point the electric field follows a square-root dependence $E \propto \sqrt{x - x_{max}}$ as would be expected from equation (2). Namely, if we define the vicinity of the interface as part of the contact then the SCL relations apply for the entire bulk of the device. This lumping procedure is similar to that performed in the context of thermionic emission over the contact barrier in the presence of the image force [42] where the region until the potential maximum is lumped with the contact.

The remaining question, in this context, is what information is lost during this lumping procedure or how valid is this procedure? It is clear that for the devices the SCL theory was developed for, which were micrometres thick, a 10–15 nm region was negligible. Also the low-voltage regime, where x_{max} is largest, is mainly important for the new high-quality low-power (voltage) LEDs. For current LEDs the layer thickness is in the range of 70–100 nm, making x_{max} account for more than 10% of the total thickness. Moreover, there is a barrier enhancement that is not accounted for (the tops of the potential curves are 0.125 and 0.34 eV for the full and dotted curves in figure 6). It is interesting to note that the extra barrier height depends on the charge density at the interface (N_0), which is essential to create the SC effect. According to equation (7) (or its equivalent), N_0 is inversely proportional to the temperature, making the barrier highest at high temperatures, thus making any activation energy at the contact effectively smaller. To conclude this paragraph, it still makes sense to use the Mott–Gurney theory for the general understanding of the device. When more detailed features are examined, one should keep in mind that this theory neglects a small diffusion-controlled region, packed with ‘self-trapped’ charges, and an extra (temperature-dependent) barrier. It may be that this lumping procedure is behind the need to add interface states in the form of traps or dipoles to better simulate experimental results [43, 44].

3.2. The effect on the time response

Figure 4 shows that the generalized Einstein relation may affect the time response of a system. Therefore, we also look into the issue of the light turn-on in LEDs and the associated mobility

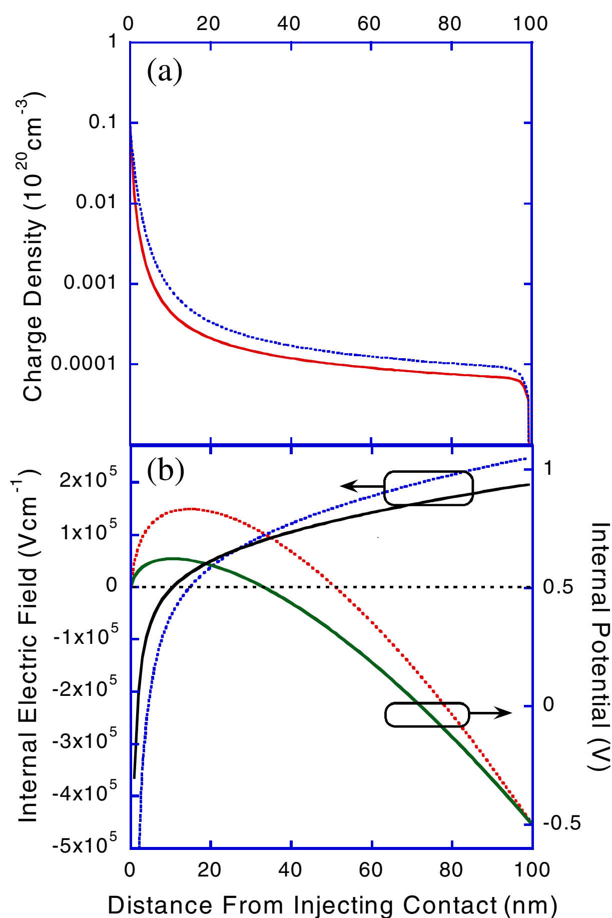

Figure 6. Calculated charge density distribution (a) and calculated internal field and potential distribution (b) for a 100 nm thick single-carrier device. The solid curves were simulated assuming the classical Einstein relation to hold and the dotted (upper) curves were calculated using the results in figure 3 for $\sigma = 7kT$.

or its extraction procedure. In [11] detailed time-domain analysis of polymer LEDs, within the standard semiconductor device-model framework, was presented, and guidelines for mobility extraction procedures were drawn. As stated in [11], the advantage of the time-domain mobility extraction method, as developed in [11], is that the mobility of the high-density part and the enhanced spreading of the carrier front are simultaneously observed. Our goal here is to show that by combining the work by Pinner *et al* [11] with the work by Roichman and Tessler [35] there is now significantly less need to resort to non-equilibrium effects to account for 'anomalous' spreading or 'too-high' diffusion constants. To illustrate the above point, we have performed calculations similar to those in [11] but including the possible effect of the width of the Gaussian DOS (figure 3) on the diffusivity parameter. Figure 7(a) shows the turn-on dynamics of a 60 nm long LED where the assumed mobility values are 1×10^{-4} and 1×10^{-5} cm^2 V^{-1} s^{-1} for holes and electrons respectively. The net applied voltage ($V_{Appl} - V_{bi}$) is assumed to be 4 V. All other parameters are as in [11]. The bottom line was calculated for a negligibly narrow DOS, where the classical Einstein relation holds, and the upper curve was calculated for a DOS width of $7kT$ (at room temperature). Using the front end

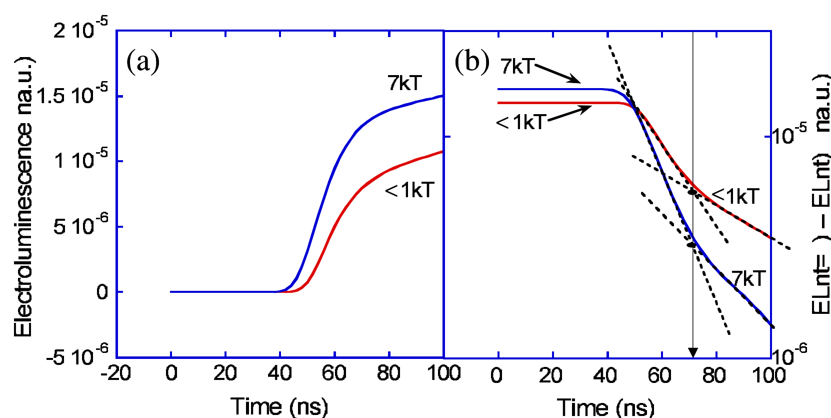

Figure 7. (a) Simulated light emission as a response to a step voltage pulse of 4 V applied at $t = 0$. The bottom curve was simulated for a material where the classical Einstein relation holds (as for $\sigma < 1kT$) and the top curve for a material having a Gaussian DOS with a width of $\sigma = 7kT$ at room temperature. Note the initial fast rise (hole arriving at the cathode) followed by a longer rise (electrons penetrate the device). (b) The data as in (a) but the curve values are extracted from the steady-state value and presented on a log scale [11]. This way the transition between hole- and electron-dominated responses is clearly visible and is marked by the vertical arrow.

of the distribution (light turn-on) to extract the mobility, the deduced hole mobility is found to be 1.9×10^{-4} and 2.2×10^{-4} cm^2 V^{-1} s^{-1} for the narrow-and wide-DOS cases, respectively. As mentioned above, such results may lead to the conclusion that in the presence of such effects it is impossible to define the mobility in an unambiguous way. However, as already pointed out in [11], the turn-on time represents only the carrier front and hence is susceptible to broadening effects and in any case does not represent the mobility (note the factor of two difference and the discussion in [11]). In figure 7(b) we plot the electroluminescence, EL(t), shown in figure 7(a), subtracted from its final value, EL($t \to \infty$), i.e. EL($t \to \infty$) − EL(t). This plot clearly reveals the presence of two distinct regions where $\log_e[\mathrm{EL}(t \to \infty) - \mathrm{EL}(t)]$ varies linearly with time. If we apply the method outlined in [11] to extract the time where the body of the hole distribution has arrived at the cathode (see the vertical arrow in figure 7(b)) we find that the arrival time is identical for the two cases (∼72 ns) and the deduced mobility is $\mu = \frac{d^2}{V\Delta t} = 1.25 \times 10^{-4}$ cm^2 V^{-1} s^{-1}, which is very close to the mobility used for both simulations (the extra 25% is due to the space-charge-enhanced electric field [1] in the bulk, that is not accounted for in such a simple expression as used here for μ). This calculation farther establishes that the method of mobility extraction developed in [11] is correct and is largely immune to fast-carrier effects. Moreover, it strengthens the notion that there is no need to resort to non-equilibrium effects in order to describe (or extract parameters from) the organic devices considered here. Other important experimental factors were discussed in detail in [11]. The self-consistent nature of the numerical model also reveals another feature of the DOS-induced diffusion enhancement. As the charge recombination is of Langevin type [10, 11, 45] (diffusion controlled), the enhanced diffusion rate enhances the exciton generation rate and hence the light output is enhanced as well.

4. Conclusions

We have shown that the nano-scale of organic devices as well as their unique electronic properties (such as Gaussian DOS) require a self-consistent analysis of the injection and

transport phenomena. The role of a Gaussian DOS is in making the material degenerate at all practical charge densities and thus affecting both steady-state and transient properties of devices of interest. We have also demonstrated that, since one has to use FD statistics and not the approximated Boltzmann statistics, not only is the transport affected but also the injection phenomena (effective barrier) are altered. It is believed that by properly accounting for the material properties (such as DOS) there is less need to introduce extrinsic factors as traps, defect states at the contact or non-equilibrium to account for the inherent non-linear behaviour of organic-material-based devices.

Acknowledgments

This research (no 56/00-11.6) was supported by The Israel Science Foundation. NT thanks the Israeli Board of Higher Education for an Allon Fellowship.

References

[1] Mott N F and Gurney R W 1940 *Electronic Processes in Ionic Crystals* (London: Oxford University Press)
[2] Ashcroft N W and Mermin N D 1988 *Solid State Physics* (New York: Holt, Rinehart and Winston)
[3] Pope M and Swenberg C E 1982 *Electronic Processes in Organic Crystals* (Oxford: Clarendon)
[4] Friend R H *et al* 1999 Electroluminescence in conjugated polymers *Nature* **397** 121–8
[5] Van der Auweraer M, Deschryver F C, Borsenberger P M and Bassler H 1994 Disorder in charge-transport in doped polymers *Adv. Mater.* **6** 199–213
[6] Scher H, Shlesinger M F and Bendler J T 1991 Time-scale invariance in transport and relaxation *Phys. Today* **44** 26–34
[7] Conwell E M and Wu M W 1997 Contact injection into polymer light-emitting diodes *Appl. Phys. Lett.* **70** 1867–9
[8] Malliaras G G and Scott J C 1999 Numerical simulations of the electrical characteristics and the efficiencies of single-layer organic light emitting diodes *J. Appl. Phys.* **85** 7426–32
[9] Davids P S, Campbell I H and Smith D L 1997 Device model for single carrier organic diodes *J. Appl. Phys.* **82** 6319–25
[10] Blom P W M, deJong M J M and Liedenbaum C 1998 Device physics of polymer light-emitting diodes *Polym. Adv. Technol.* **9** 390–401
[11] Pinner D J, Friend R H and Tessler N 1999 Transient electroluminescence of polymer light emitting diodes using electrical pulses *J. Appl. Phys.* **86** 5116–30
[12] Campbell A J, Bradley D D C, Antoniadis H, Inbasekaran M, Wu W S W and Woo E P 2000 Transient and steady-state space–charge-limited currents in polyfluorene copolymer diode structures with ohmic hole injecting contacts *Appl. Phys. Lett.* **76** 1734–6
[13] Kraft A, G A C and H A B 1998 Electroluminescent conjugated polymers—seeing polymers in a new light *Angew. Chem. Int. Edn* **37** 402–28
[14] Heeger A J 2001 Semiconducting and metallic polymers: the fourth generation of polymeric materials (Nobel lecture) *Angew. Chem. Int. Edn* **40** 2591–611
[15] Pei Q B, Yu G, Zhang C, Yang Y and Heeger A J 1995 Polymer light-emitting electrochemical-cells *Science* **269** 1086–8
[16] Ho P K H, Thomas D S, Friend R H and Tessler N 1999 All-polymer optoelectronic devices *Science* **285** 233–6
[17] Yoffe A D 1993 Low-dimensional systems—quantum-size effects and electronic-properties of semiconductor microcrystallites (zero-dimensional systems) and some quasi-2-dimensional *Adv. Phys.* **42** 173–266
[18] Bassler H 1993 Charge transport in disordered organic photoconductors *Phys. Status Solidi* b **175** 15–56
[19] Scher H and Montroll E M 1975 Anomalous transit-time dispersion in amorphous solids *Phys. Rev.* B **12** 2455–77
[20] Hartenstein B, Bassler H, Jakobs A and Kehr K W 1996 Comparison between multiple-trapping and multiple hopping transport in a random medium *Phys. Rev.* B **54** 8574–9
[21] Horsche E M, Haarer D and Scher H 1987 Transition from dispersive to nondispersive transport: photoconduction of polyvinylcarbazole *Phys. Rev.* B **35** 1273–80
[22] Gu Q, Schiff E A, Grebner S, Wang F and Schwarz R 1996 Non-Gaussian transport measurements and the Einstein relation in amorphous silicon *Phys. Rev. Lett.* **76** 3196–9

[23] Campbell A J, Bradley D D C and Antoniadis H 2001 Dispersive electron transport in an electroluminescent polyfluorene copolymer measured by the current integration time-of-flight method *Appl. Phys. Lett.* **79** 2133–5

[24] Blom P W M and Vissenberg M 1998 Dispersive hole transport in poly(p-phenylene vinylene) *Phys. Rev. Lett.* **80** 3819–22

[25] Borsenberger P M, Magin E H, Vanderauweraer M and Deschryver F C 1993 The role of disorder on charge-transport in molecularly doped polymers and related materials *Phys. Status Solidi* a **140** 9–47

[26] Meskers S C J, Hubner J, Oestreich M and Bassler H 2001 Dispersive relaxation dynamics of photoexcitations in a polyfluorene film involving energy transfer: experiment and Monte Carlo simulations *J. Phys. Chem.* B **105** 9139–49

[27] Pautmeier L, Richert R and Bassler H 1991 Anomalous time-independent diffusion of charge-carriers in a random potential under a bias field *Phil. Mag.* B **63** 587–601

[28] Martens H C F, Huiberts J N and Blom P W M 2000 Simultaneous measurement of electron and hole mobilities in polymer light-emitting diodes *Appl. Phys. Lett.* **77** 1852–4

[29] Wright G T 1966 Transit time effects in the space-charge-limited silicon microwave diode *Solid-state electronics* **9** 1

[30] Roichman Y and Tessler N 2002 Generalized Einstein relation for disordered semiconductors—implications for device performance *Appl. Phys. Lett.* **80** 1948–50

[31] Gill W D 1972 Drift mobilities in amorphous charge-transfer complexes of trinitrofluorenone and poly-n-vinylcarbazole *J. Appl. Phys.* **43** 5033

[32] Bassler H, Schonherr G, Abkowitz M and Pai D M 1982 Hopping transport in prototypical organic glasses *Phys. Rev.* B **26** 3105–13

[33] Arkhipov V I, Wolf U and Bassler H 1999 Current injection from metal to disordered hopping system. II. Comparison between analytic theory and simulation *Phys. Rev.* B **59** 7514–20

[34] Richert R, Pautmeier L and Bassler H 1989 Diffusion and drift of charge-carriers in a random potential—deviation from Einstein law *Phys. Rev. Lett.* **63** 547–50

[35] Roichman Y and Tessler N 1966 Generalized Einstein-relation for disordered semiconductors—implications for device performance *Appl. Phys. Lett.* **9** 1

[36] Morse P M and Feshbach H 1953 *Methods of Theoretical Physics* (New York: McGraw-Hill)

[37] Campbell A J, Weaver M S, Lidzey D G and Bradley D D C 1998 Bulk limited conduction in electroluminescent polymer devices *J. Appl. Phys.* **84** 6737–46

[38] Scott J C, Ramos S and Malliaras G G 1999 Transient space–charge-limited current measurements of mobility in a luminescent polymer *J. Imaging Sci. Technol.* **43** 233–6

[39] Alvarado S F, Rossi L, Muller P, Seidler P F and Riess W 2001 STM-excited electroluminescence and spectroscopy on organic materials for display applications *IBM J. Res. Dev.* **45** 89–100

[40] Malliaras G G and Scott J C 1998 The roles of injection and mobility in organic light emitting diodes *J. Appl. Phys.* **83** 5399–403

[41] Crone B K, Davids P S, Campbell I H and Smith D L 2000 Device model investigation of bilayer organic light emitting diodes *J. Appl. Phys.* **87** 1974–82

[42] Sze S M 1981 *Physics of Semiconductor Devices* (New York: Wiley)

[43] Baldo M A and Forrest S R 2001 Interface-limited injection in amorphous organic semiconductors *Phys. Rev.* B **64** 085201

[44] Lupton J M, Nikitenko V R, Samuel I D W and Bassler H 2001 Time delayed electroluminescence overshoot in single layer polymer light-emitting diodes due to electrode luminescence quenching *J. Appl. Phys.* **89** 311–17

[45] Albrecht U and Bassler H 1995 Langevin-type charge-carrier recombination in a disordered hopping system *Phys. Status Solidi* b **191** 455–9